OPEN

Correspondence and
requests for materials
should be addressed to
H.Y.Y. (yu.hy@sustc.
edu.cn) or H.B.S.
(hbsu@ntu.edu.sg)

The transport properties of oxygen vacancy-related polaron-like bound state in HfO$_x$

Zhongrui Wang[1], HongYu Yu[2] & Haibin Su[1]

[1]Nanyang Technological University, Singapore 639798, [2]South University of Science and Technology of China, China 518055.

The oxygen vacancy-related polaron-like bound state migration in HfO$_x$ accounting for the observed transport properties in the high resistance state of resistive switching is investigated by the density functional theory with hybrid functional. The barrier of hopping among the threefold oxygen vacancies is strongly dependent on the direction of motion. Especially, the lowest barrier along the <001> direction is 90 meV, in agreement with the experimental value measured from 135 K to room temperature. This hopping mainly invokes the z-directional motion of hafnium and threefold oxygen atoms in the vicinity of the oxygen vacancy resulted from the synergized combination of coupled phonon modes. In the presence of ($\bar{1}11$) surface, the lowest barrier of hopping between the surface oxygen vacancies is 360 meV along the <101> direction, where the significant surface perpendicular motion of hafnium and twofold oxygen atoms surrounding the oxygen vacancy is identified to facilitate this type of polaron-like bound state migration. Thus, the migration on the surfaces could be more important at the high temperature.

R esistive switching in thin film devices attracts great interests for potential applications in future non-volatile memories[1,2]. The monoclinic phase of HfO$_x$ (m-HfO$_x$) is a material of particular importance to resistive switching memories, which exhibits reversible metal-insulator transitions in operations[3,4]. Oxygen vacancies have been widely speculated to be responsible for the valence change type bipolar resistive switching in oxides[5,6]. Spectroscopic ellipsometer measurements have revealed that oxygen vacancies are dominant native defects in m-HfO$_x$[7]. The observed switching process in m-HfO$_x$ is likely due to the percolation of oxygen vacancies[8]. In the high resistance state, the electronic state associated with doped oxygen vacancies tends to localize within the mobility gap, which possesses experimental significances of polaron-like transport as revealed by the field and temperature dependent dielectric loss measurements[8]. And the observed thermal activation energy transition at half of the Debye temperature (E$_A$ ~ 50 meV at T > θ/2) is consistent with the prediction based on the kinetics of polaronic motion by Schnakenberg[8–10].

The presence of polarons in transition metal oxides are facilitated by the significant electron-phonon interaction[11,12]. The details of polaron transport are reviewed by Holstein[13,14], Marcus[15], Emin[16], Friedman[17], Alexandrov[18], Austin and Mott[10], Ross et al.[19] The intrinsic polaron state has been proposed in m-HfO$_2$ without invoking oxygen vacancies[20,21]. For oxygen deficient HfO$_x$, the trapping of extra electrons by defect states promotes electron-lattice coupling, which leads to the formation of polaron-like bound states in m-HfO$_x$[22]. Density functional calculations of polaron-like bound state trapping on oxygen vacancies of m-HfO$_x$ were reported with hybrid functionals approaches[23–25]. Recently, continuous calculation by using density functional theory of the total energy along the entire migration pathway has been reported of accurate predictions of activation energy[20,26–28]. Despite intensive studies of polaron-like carrier trapping in m-HfO$_x$, the detailed migration pathway of oxygen vacancy-related polaron-like bound states in m-HfO$_x$ in either bulk lattice or presence of surfaces is yet to be clarified, which is of great importance for interpreting the observed transport behaviours in m-HfO$_x$ based resistive switching memory. Besides, the influence of lattice on the polaron-like bound state hopping is unclear in m-HfO$_x$. Here we study the high resistance state transport in oxygen deficient m-HfO$_x$ resistive memory leveraged on the previous studies on charge migration[26,27,29,30]. Computational evidence is presented for the motion of oxygen vacancy-related polaron-like bound state in m-HfO$_x$. Using hybrid functional based conjugate gradient refined linear and quadratic synchronous transit schemes[31], we characterize the anisotropic hopping barriers for polaron-like bound states jumping between equivalent threefold oxygen vacancies along lattice vectors. The value of the lowest barrier is in consistency with experimental measurement from 135 K to room temperature. Projected phonon density of states has been calculated, indicating large vibration with
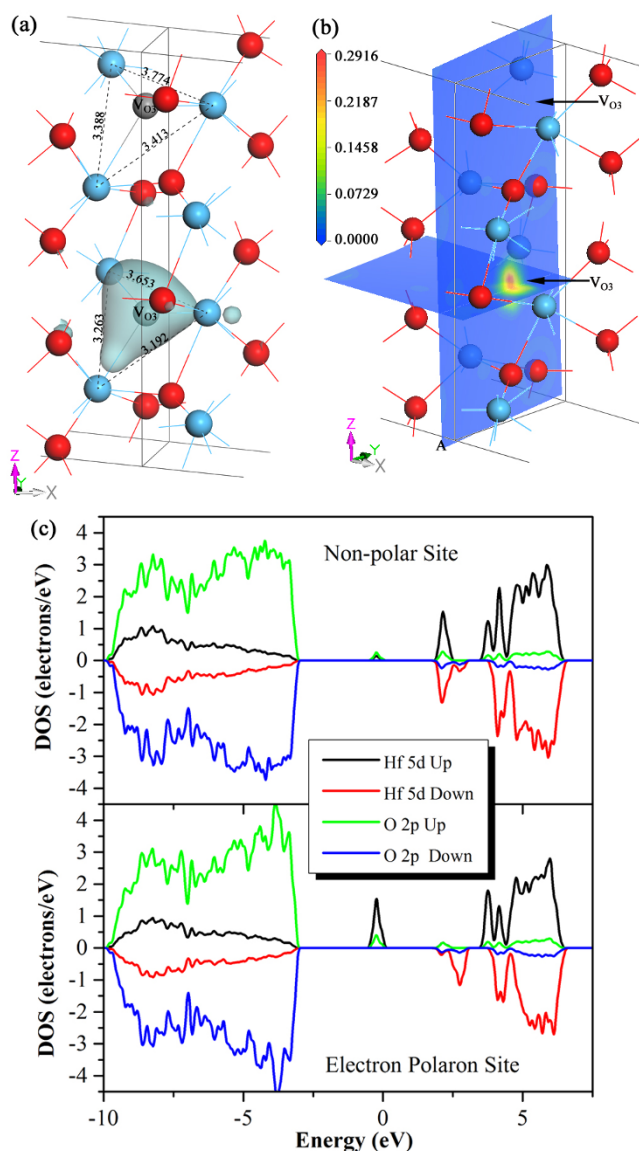
1

Table 1 | Calculated spin distribution over vacancy neighboring hafnium atoms

Lower vacancy site ($\hbar$)	Upper vacancy site ($\hbar$)
0.11	0.01
0.16	0.01
0.22	0

Figure 1 | (a) The optimized $1 \times 1 \times 2$ lattice with two threefold oxygen vacancies. Hafnium, oxygen atom, and vacancy are represented by blue, red and grey balls, respectively. An isosurface (Isovalue = 0.05 Å^{-3}) shows the spin distribution. The black dashed line and labels indicate inter-atomic distances in angstroms between the vacancy-neighbouring hafnium atoms. The spin mainly localizes on the lower oxygen vacancy site. (b) (100) and (001) slice view of the electron localization function calculated from valence electrons of the configuration in (a). The arrows point to the original positions of the oxygen vacancies. An attractor is located at the site of the lower vacancy while the value of electron localization function of the upper site is close to zero. (c) Atom projected density of states for the upper unit cell (non-polar site) and lower unit cell (polar site) in (a). Fermi level is set to be zero eV. The polaron-like bound state is mainly composed of Hf $5d$ atomic orbital.

Results

The imperfect treatment of self-interaction in density functional theory tends to overly delocalize d electrons and yield an under-estimation of the bandgap[32]. Recently functionals such as sX, PBE0 and B3LYP have been used in the study of oxygen vacancies in HfOx[23–25]. By including a fraction of exact exchange, the B3LYP functional in our calculation, which correctly predicts stoichiometric monoclinic HfO2 (a = 5.00 Å, b = 5.06 Å, c = 5.18 Å, β = 100.1°) to be an insulator with a gap of 6.2 eV in good agreement with previous reports[7,23–25]. Introducing oxygen vacancies with positive charge creates t_{2g} molecular orbitals with σ symmetry to hafnium-vacancy axis[33]. Here, each supercell contains two m-HfO2 unit cells with oxygen vacancies at equivalent positions. Although the threefold oxygen vacancy has strong tendency of retaining +2 charge state[23–25], the total charge per supercell is set to be +3 to model the effect of electron reservoirs existed during the operation of RRAM devices.

Structure-wise, with 12.5% concentration of fourfold oxygen vacancies, the lattice is transformed into orthorhombic phase (a = 10.58 Å, b = 4.20 Å, c = 4.27 Å). Subsequent transition to tetragonal phase is observed with increasing non-stoichiometry, consistent with the report of Xue et al.[34] On the other hand, threefold oxygen vacancies only transform the structure into triclinic phase. The structural transformation resulting from the increase of the oxygen vacancy content is also observed in other transition metal oxides including cuprates[35]. The localization feature of the polaron-like bound state needs judicious correction of self-interaction error. Localization of the polaron-like bound state is studied with the exchange limit on both types of oxygen vacancies. For fourfold oxygen vacancies, the charge density computed by exact exchange is localized on one oxygen vacancy while the charge is distributed over both vacancies when computed with B3LYP functional, which suggests that the localization in fourfold oxygen vacancies requires much stringent treatment of the self-interaction error. However, the charge is localized on threefold oxygen vacancies when computed with B3LYP, which is consistent with the result by exact exchange. Moreover, threefold oxygen vacancies are more energetically favourable. Thus, the main study focuses on threefold oxygen vacancies.

The oxygen vacancy in m-HfOx induces changes of the local lattice structure. In the 12.5% concentration case, after B3LYP optimization, phase transformation takes place in the $1 \times 1 \times 2$ supercell, which transforms the lattice to triclinic phase. (a = 4.71 Å, b = 4.95 Å, c = 9.60 Å, α = 90.9°, β = 95.2°, γ = 89.7°) The localization of the polaron-like bound state shown in Figure 1(a) is accompanied by displacement of three neighbouring hafnium atoms by ~0.2 Å towards each other, on average, about 10% of the O-Hf distance. In this case, about 50% of the electron spin density is localized pre-dominantly on three hafnium ions sharing the missing threefold oxygen atoms, similar to that of the polaron in m-HfO2[20]. The spin distribution, listed in Table 1, is asymmetrical among the hafnium ions. Electron localization function has been calculated from the valence electrons as an approximation to the all-orbital electron localization function. (Note that electron localization function values from CASTEP do not span the full range from 0 to 1.) Irreducible f-localization domain, as shown in Figure 1(b), could be defined by comprising the single attractor located at the position of the lower oxygen vacancy. As a contrast, the calculated electron localization function in the vicinity of the higher oxygen vacancy is close to zero,

vacancy-neighbouring threefold oxygen and hafnium atoms. In the presence of ($\bar{1}11$) surface, the kinetic barrier of the symmetrical hopping is significantly higher than that of the hopping in the bulk. Surface phonon modes, localizing on vacancy-neighbouring hafnium and twofold oxygen atoms, are identified to facilitate this hopping. The experimentally observed barrier in the high temperature range from 320 K to 400 K is clearly about two to three times larger than that in low temperature. Thus, this work suggests that surface polaron migration may be important to the observed transport at high temperature.

Table 2 | Calculated lowest polaron-like bound state migration barriers between threefold oxygen vacancies in the equivalent sites in the bulk HfO_x along <100>, <010> and <001> directions

Direction	Hopping Barrier (meV)	Distance (Å)
<100>	661.19	4.62
<010>	2814.79	4.76
<001>	90.47	4.80

which confirms the asymmetrical spin localization. Figure 1(b) shows the atomic projected density of states. The polaron-like bound state occupies the spin-up state at the Fermi level, and is mainly composed of hafnium 5d orbitals on which the electron is localized. The localization splits the original degenerate bandgap states induced by oxygen vacancies by pushing up the un-occupied spin-down state 2 eV above the Fermi level. Weak coupling between vacancies leads to the small band dispersion (~0.26 eV) of the polaron-like bound state, implying electron localization in the low density limit[36].

The polaron-like bound state migration is strongly dependent on the direction of motion in bulk HfO_x. Polaron-like bound states migrate along three different directions (i.e. <100>, <010>, and <001>) between two equivalent neighbouring vacancies. The hopping direction dependent barriers unravel the anisotropic characteristics in transport process as presented in Table 2. Austin and Mott have proposed that the relationship between polaron hopping activation energy and distance is $W_H = \frac{e^2}{4} \left(\frac{1}{\kappa_\infty} - \frac{1}{\kappa} \right) \left(\frac{1}{r_P} - \frac{1}{R} \right)$, where e is the electron charge, κ_∞ / κ is the high-frequency/static dielectric constant, r_p is the polaron radius, and R is the distance between hopping centres[10]. However, the application of this formula in anisotropic transport needs more caution. In Figure 2(a), the transition state of <100> directional migration is accompanied with remarkable lattice distortions. Appreciable changes of bond length are observed, as shown in Figure 2(a). Compared to the charge in the initial localized state, the charge in the same region is reduced when in the transition state. This leads to the increment of the inter-atomic separation between hafnium atoms neighbouring the lower oxygen

vacancy where the charge is originally trapped. So, the chemical bonding between hafnium and oxygen has covalent component besides the commonly discussed ionic nature. Similar analysis is performed for the hopping along <010> and <001> directions. Hopping along <010> direction experiences the highest barrier as shown in Figure 2(b), where significant changes in bond length are identified between threefold oxygen and hafnium atoms. When hopping is along <001> direction, the changes in bond lengths are much smaller mainly involving atoms near the vacancies as shown in Figure 2(c). The computed lowest activation energy is 90 meV along the <001> direction, which is in agreement with the measured thermal activation energy of 87 meV observed by Compagnoni et al. in the temperature range from 135 K to room temperature[37]. Ramo et al. have reported that the electron polaron migration barrier in perfect HfO_2 is 50 meV by linear extrapolation approach[20]. Compared to hopping of polaron, polaron-like bound state migration is facing a relatively larger barrier.

We have calculated the projected phonon density of states, shown in Figure 3 (a), of the configuration with lowest hopping barrier along <001> direction. Projecting the displacement vector, the coordinate difference between transition state and reactant factored by the square root of atomic mass, onto the phonon eigenvectors at Γ point, the eigenvalues of the modes with top ten projections span the energy range from 8 to 45 meV. By inspecting the eigenvectors, the vibration of the mode with largest projection is polarized perpendicular to z-axis, mainly concerning the motion of hafnium atoms and threefold oxygen atoms. Higher order effect of the phonon eigenvectors are also estimated by varying the amplitude of the displacements, where the modes could be grouped based on the inter-mode anharmonic coupling. The transition state displacement is mainly a superposition of two groups of phonon modes, one concerning the modes localized on hafnium atoms with energy from 8 to 14 meV while the other consisting of motion of threefold oxygen atoms parallel to z-axis (i.e. O3 and O4) with energy from 24 to 45 meV, as illustrated in the inset of Figure 3(a) and Figure 3(b). The synergized combination of strongly coupled phonon modes play important roles in the migration may closely relate to the migration of polaron along the <001> direction.
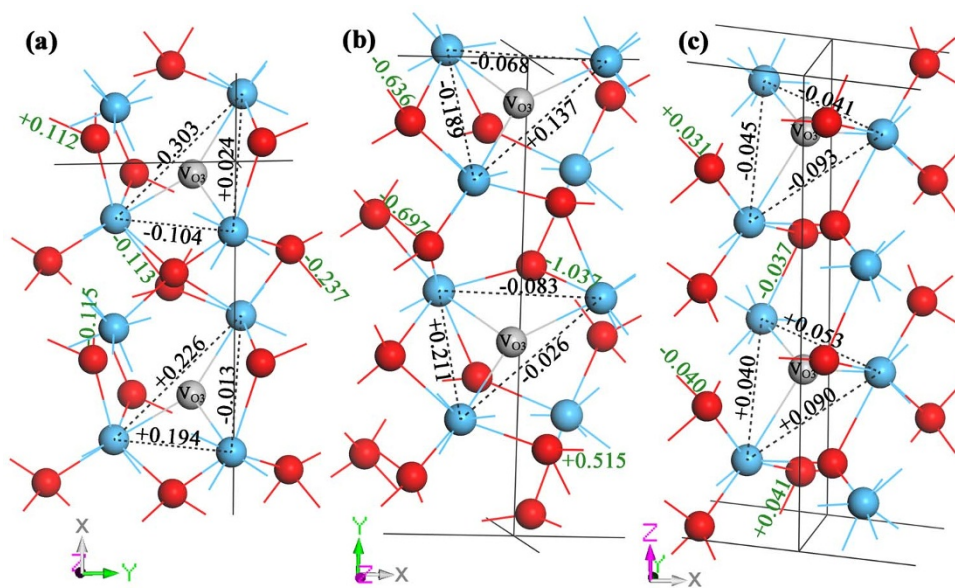
Figure 2 | Calculated transition states of (a) <100> directional hopping in a 2 × 1 × 1 lattice with two threefold oxygen vacancies (b) <010> directional hopping in a 1 × 2 × 1 lattice with two threefold oxygen vacancies (c) <001> directional hopping in a 1 × 1 × 2 lattice with two threefold oxygen vacancies. The polaron-like bound states are originally localized on lower oxygen vacancies. The black dashed lines and labels indicate changes of inter-atomic distances in angstroms between the vacancy-neighbouring hafnium atoms. Green labels are major bond length changes given in angstroms.
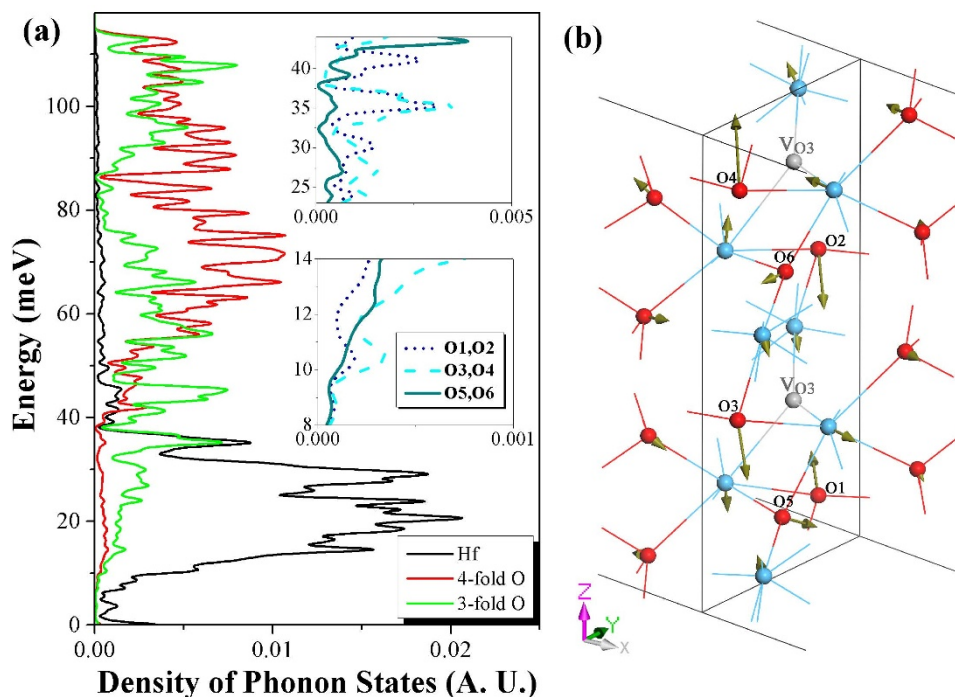
Figure 3 | (a) Calculated atom projected phonon density of states of the $1 \times 1 \times 2$ HfO$_x$ lattice in Figure 1. The lower inset shows the zoomed view from 8 meV to 14 meV while the upper inset shows the zoomed view from 23 to 43 meV, which correspond to the contributions of the labelled threefold oxygen atoms in (b). (b) Illustration of combined phonon packets. Arrows are the superposition of the two dominant phonon groups of coupled modes where the vibration is mainly with hafnium and threefold oxygen atoms.

McKenne and Shluger have found that grain boundaries act as sinks for oxygen vacancies so percolation paths are preferentially located along grain boundaries[38]. Thus it is interesting to investigate the polaron-like bound state migration pathways in the vicinity of the boundaries. In this work, we focus on the migration dynamics near the ($\bar{1}$11) surface which possesses the lowest surface energy (1.105 J/m^2) among various low index surfaces[8]. For simplicity, symmetrical hopping between equivalent sites on ($\bar{1}$11) surfaces are investigated along either <110> or <101> direction with sixteen different paths. By using the slab model with two layers of HfO$_x$ structure (a = 6.27 Å, b = 13.76 Å), the lowest activation barrier is found to be 360 meV along the <101> direction over 6.24 Å as given in Table 3. Experimentally, the trap depth in HfO$_x$, which presumes a Poole-Frenkel emission model, was found to fall in the range from 210 meV to 350 meV in the elevated temperature region from 300 K to 400 K[39,40]. As Poole-Frenkel behaviours are likely to have an origin of small polaron hopping[8,41], it is very likely that polaron-like bound state hopping near surface dominates over the bulk hopping in the high temperature region due to oxygen vacancy segregation near surfaces and the subsequent suppression of inter-grain coherent linkage.

Figure 4 (a) is the projected phonon density of states. Projecting the displacement vector onto the phonon eigenvectors at Γ-point, the modes with largest projections are below 48 meV, especially in the range from 7 to 20 meV. The dominant contribution to branches with large projections comes from the vibration of hafnium and twofold oxygen atoms neighbouring oxygen vacancies, as shown in Figure 4(a). Analysis of the phonon eigenvector with largest projection reveals the vibration is mainly polarized perpendicular to the surface. It is also noted that relatively large projection comes from branches with energy 45 meV to 48 meV, passing through the forbidden regions between the bulk continuums at non-zero q-points in Figure 4(b), which reveals the importance of surface modes to polaron hopping along the surface[42]. These branches are also noticed to be almost dispersionless along the symmetry directions due to the

very large mass difference between hafnium and oxygen atoms. We have also computed the phonon structure of the ($\bar{1}$11) surface without oxygen vacancies and strong resemblance is found in dispersion. An exception, however, is that the branches appearing in the forbidden region between the acoustic and optical bulk phonon modes are drastically changed due to oxygen vacancies induced surface relaxation. Like the bulk case, anharmonic coupling between modes is estimated by varying the amplitude used in the finite displacement method. The displacement of the transition states is mainly composed of the group of coupled modes in the energy range from 7 to 13 meV, as shown in Figure 4(c), localized on the hafnium and twofold oxygen atoms in the vicinity of the oxygen vacancies.

Discussion

The oxygen vacancy-related polaron-like bound state is clearly localized in the high resistance state of m-HfO$_x$ investigated by the density functional theory with the hybrid functional including proper portion of non-local exact exchange. Anisotropic migration barriers are found for polaron-like bound state hopping between the equivalent threefold oxygen vacancies. The lowest barrier of threefold oxygen vacancy-related polaron-like bound state along the <001> direction is 90 meV, in agreement with the experimental value. The z-directional motion of the neighbouring hafnium and threefold oxygen atoms are identified to play important roles in the hopping of polaron-like bound state. In the presence of ($\bar{1}$11) surface, lowest migration hopping path is

Table 3 | Calculated lowest polaron-like bound state migration barriers between threefold oxygen vacancies in the equivalent sites on the ($\bar{1}$11) surface of HfO$_x$ along <110> and <101> directions

Direction	Hopping Barrier (meV)	Distance (Å)
<110>	519.70	6.88
<101>	360.93	6.24
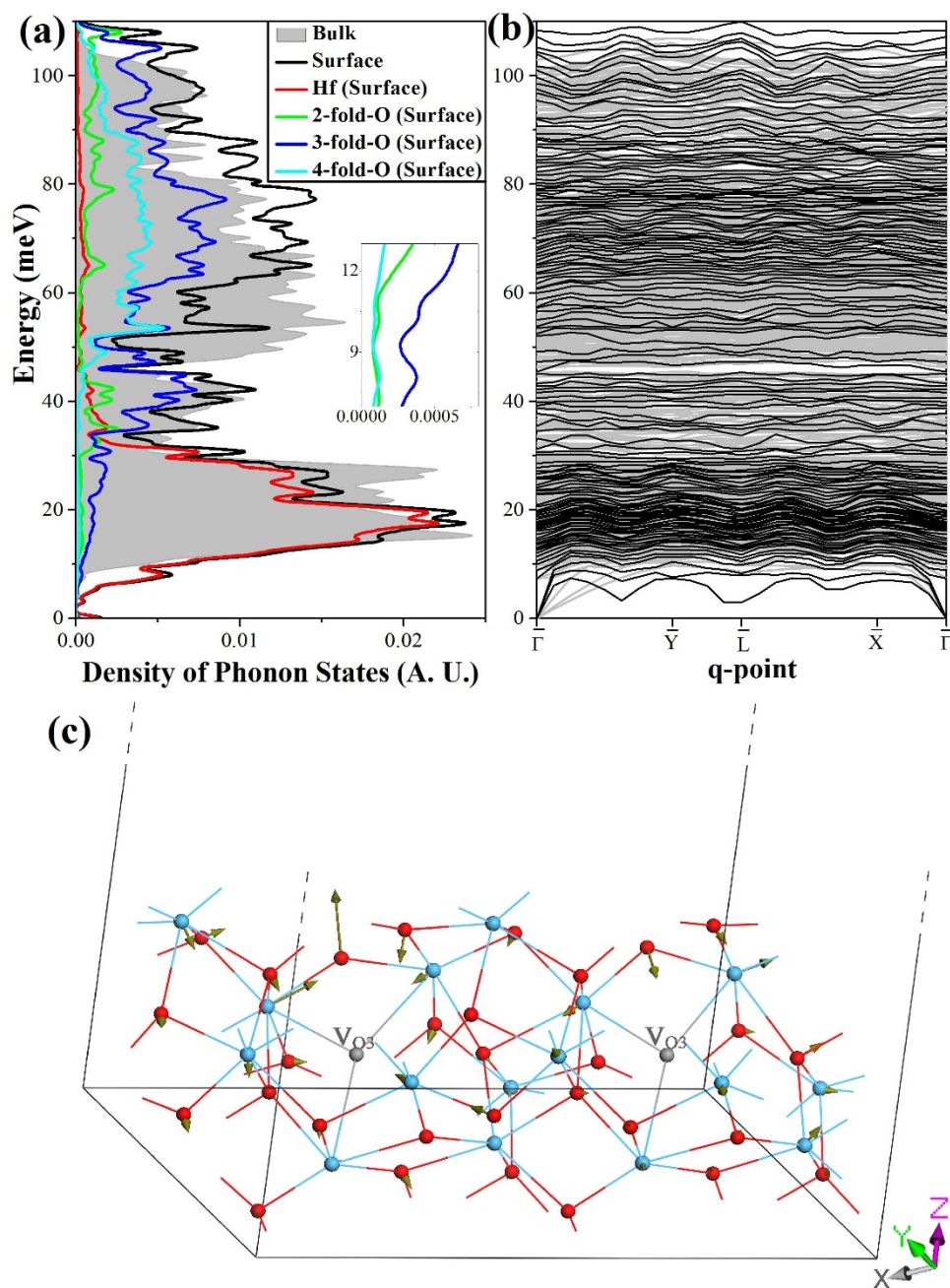
Figure 4 | (a) Calculated atom projected phonon density of states and (b) phonon dispersion of ($\bar{1}11$) HfO$_x$ 2-layer vacuum slab model with lowest symmetrical migration energy along <101> direction. The projected bulk phonon dispersion of HfO$_x$ is shown by the hatched region. The branches within energy range from 45 to 48 meV pass through the forbidden regions between the bulk continuums at non-zero q-points, representing surface modes. (c) Illustration of the dominant phonon packet. Arrows are the superposition of coupled modes where the vibration is mainly with the vacancy-neighbouring hafnium and twofold oxygen atoms.

found to be along <101> direction with displacements mainly invoking the surface perpendicular motion of phonon modes localized on the vacancy-neighbouring hafnium and twofold oxygen atoms. The present work based on the oxygen vacancy-related polaron-like bound state sheds light on the microscopic nature of the transport process in the high resistance state of m-HfO$_x$ resistive memory devices.

Method
Here we use the plane wave pseudo-potential code CASTEP[43], with norm-conserving pseduopotentials method aided by B3LYP functional and an energy cutoff at 450 eV. The calculation is performed by using the spin polarized density functional theory[44]. For cell optimization, the supercell parameters are optimized in their charge states

using PBE version of GGA with norm-conserving pseduopotentials. The geometry is further optimized by B3LYP method. The transition state search is implemented by the combination of linear synchronous transit and quadratic synchronous transit schemes[45] with 0.1 eV/Å convergence threshold for the root mean square forces on the atoms[31,46,47]. K-point convergence test has been done and 5 irreducible k-points are used in sampling. For transition state search related calculations, only Γ point is used to reduce computational cost. Phonon dispersion and density of states calculation are computed by the finite displacement method implemented in CASTEP[48].

1. Beck, A. *et al.* Reproducible switching effect in thin oxide films for memory applications. *Appl. Phys. Lett.* **77**, 139–141 (2000).
2. Rossel, C., Meijer, G. I., Brémaud, D. & Widmer, D. Electrical current distribution across a metal–insulator–metal structure during bistable switching. *J. Appl. Phys.* **90**, 2892–2898 (2001).

3. Zhang, H. *et al.* Gd-doping effect on performance of HfO₂ based resistive switching memory devices using implantation approach. *Appl. Phys. Lett.* **98**, 042105 (2011).

4. Govoreanu, B. *et al.* 10×10 nm² Hf/HfOₓ crossbar resistive RAM with excellent performance, reliability and low-energy operation. *Electron Devices Meeting (IEDM), 2011 IEEE International*, 31.36.31–31.36.34 (2011).

5. Gao, B. *et al.* Unified physical model of bipolar oxide-based resistive switching memory. *IEEE Electron Device Lett.* **30**, 1326–1328 (2009).

6. Waser, R., Dittmann, R., Staikov, G. & Szot, K. Redox-based resistive switching memories - nanoionic mechanisms, prospects, and challenges. *Adv. Mater.* **21**, 2632–2663 (2009).

7. Takeuchi, H., Ha, D. & King, T.-J. Observation of bulk HfO₂ defects by spectroscopic ellipsometry. *J. Vac. Sci. Technol., A* **22**, 1337–1341 (2004).

8. Wang, Z. *et al.* Transport properties of HfO₂₋ₓ based resistive-switching memories. *Phys. Rev. B* **85**, 195322 (2012).

9. Schnakenberg, J. Polaronic impurity hopping conduction. *Phys. Status Solidi B* **28**, 623–633 (1968).

10. Austin, I. G. & Mott, N. F. Polarons in crystalline and non-crystalline materials. *Adv. Phys.* **50**, 757–812 (2001).

11. Elliott, S. *The Physics and Chemistry of Solids.* (Wiley, 1998).

12. Cox, P. A. *The electronic structure and chemistry of solids.* (Oxford University Press, 1987).

13. Holstein, T. Studies of polaron motion: Part I. The molecular-crystal model. *Ann. Phys.* **8**, 325–342 (1959).

14. Holstein, T. Studies of polaron motion: Part II. The "small" polaron. *Ann. Phys.* **8**, 343–389 (1959).

15. Marcus, R. A. Electron transfer reactions in chemistry. Theory and experiment. *Rev. Mod. Phys.* **65**, 599–610 (1993).

16. Emin, D. & Holstein, T. Studies of small-polaron motion IV. Adiabatic theory of the Hall effect. *Ann. Phys.* **53**, 439–520 (1969).

17. Friedman, L. & Holstein, T. Studies of polaron motion: Part III: The Hall mobility of the small polaron. *Ann. Phys.* **21**, 494–549 (1963).

18. Alexandrov, A. S. & Mott, N. F. Bipolarons. *Rep. Prog. Phys.* **57**, 1197–1288 (1994).

19. Rosso, K. M. & Dupuis, M. Electron transfer in environmental systems: a frontier for theoretical chemistry. *Theor. Chem. Acc.* **116**, 124–136 (2005).

20. Muñoz Ramo, D., Shluger, A., Gavartin, J. & Bersuker, G. Theoretical prediction of intrinsic self-trapping of electrons and holes in monoclinic HfO₂. *Phys. Rev. Lett.* **99**, 155504 (2007).

21. McKenna, K. P. *et al.* Two-dimensional polaronic behavior in the binary oxides m-HfO₂ and m-ZrO₂. *Phys. Rev. Lett.* **108**, 116403 (2012).

22. Gavartin, J. L., Ramo, D. M., Shluger, A. & Bersuker, G. Polaron-like charge trapping in oxygen deficient and disordered HfO₂: theoretical insight. *ECS Trans.* **3**, 277–290 (2006).

23. Xiong, K., Robertson, J., Gibson, M. C. & Clark, S. J. Defect energy levels in HfO₂ high-dielectric-constant gate oxide. *Appl. Phys. Lett.* **87**, 183505 (2005).

24. Broqvist, P. & Pasquarello, A. Oxygen vacancy in monoclinic HfO₂: A consistent interpretation of trap assisted conduction, direct electron injection, and optical absorption experiments. *Appl. Phys. Lett.* **89**, 262904 (2006).

25. Muñoz Ramo, D., Gavartin, J., Shluger, A. & Bersuker, G. Spectroscopic properties of oxygen vacancies in monoclinic HfO₂ calculated with periodic and embedded cluster density functional theory. *Phys. Rev. B* **75**, 205336 (2007).

26. Maxisch, T., Zhou, F. & Ceder, G. Ab initio study of the migration of small polarons in olivine LiₓFePO₄ and their association with lithium ions and vacancies. *Phys. Rev. B* **73**, 104301 (2006).

27. Deskins, N. A. & Dupuis, M. Intrinsic Hole Migration Rates in TiO2 from Density Functional Theory. *J. Chem. Phys. C* **113**, 346–358 (2008).

28. Wolf, M. J., McKenna, K. P. & Shluger, A. L. Hole trapping at surfaces of *m*-ZrO₂ and *m*-HfO₂ nanocrystals. *J. Chem. Phys. C* **116**, 25888–25897 (2012).

29. Deskins, N. & Dupuis, M. Electron transport via polaron hopping in bulk TiO₂: A density functional theory characterization. *Phys. Rev. B* **75**, 195212 (2007).

30. McKenna, K. P. & Blumberger, J. Crossover from incoherent to coherent electron tunneling between defects in MgO. *Phys. Rev. B* **86** (2012).

31. Govind, N. *et al.* A generalized synchronous transit method for transition state location. *Comp. Mater. Sci.* **28**, 250–258 (2003).

32. Liechtenstein, A. I. & Zaanen, J. Density-functional theory and strong interactions: Orbital ordering in Mott-Hubbard insulators. *Phys. Rev. B* **52**, R5467–R5470 (1995).

33. Coey, J. *et al.* Magnetism in hafnium dioxide. *Phys. Rev. B* **72**, 024450 (2005).

34. Xue, K.-H., Blaise, P., Fonseca, L. R. C. & Nishi, Y. Prediction of Semimetallic Tetragonal Hf₂O₃ and Zr₂O₃ from First Principles. *Phys. Rev. Lett.* **110** (2013).

35. Su, H. B., Welch, D. O. & Wong-Ng, W. Strain effects on point defects and chain-oxygen order-disorder transition in 123 cuprate compounds. *Phys. Rev. B* **70** (2004).

36. Zallen, R. *The physics of amorphous solids.* (Wiley, 1983).

37. Compagnoni, C. M. *et al.* Temperature dependence of transient and steady-state gate currents in HfO₂ capacitors. *Appl. Phys. Lett.* **89**, 103504 (2006).

38. McKenna, K. & Shluger, A. The interaction of oxygen vacancies with grain boundaries in monoclinic HfO₂. *Appl. Phys. Lett.* **95**, 222111 (2009).

39. Ribes, G. *et al.* Origin of Vt instabilities in high-k dielectrics Jahn-Teller effect or oxygen vacancies. *IEEE Trans. Dev. Mater. Reliab.* **6**, 132–135 (2006).

40. Southwick, R. G. *et al.* Limitations of Poole–Frenkel conduction in bilayer HfO₂/SiO₂ MOS devices. *IEEE Trans. Dev. Mater. Reliab.* **10**, 201–207 (2010).

41. Emin, D. Generalized adiabatic polaron hopping: Meyer-Neldel compensation and Poole-Frenkel behavior. *Phys. Rev. Lett.* **100**, 166602 (2008).

42. Fritsch, J. & Schröder, U. Density functional calculation of semiconductor surface phonons. *Phys. Rep.* **309**, 209–331 (1999).

43. Clark, S. J. *et al.* First principles methods using CASTEP. *Z. Kristallogr.- Cryst. Mater.* **220**, 567–570 (2005).

44. Hadacek, N. *et al.* Magnetic properties of HfO₂ thin films. *J. Phys.: Condens. Matter* **19**, 486206 (2007).

45. Halgren, T. A. & Lipscomb, W. N. The synchronous-transit method for determining reaction pathways and locating molecular transition states. *Chem. Phys. Lett.* **49**, 225–232 (1977).

46. Bell, S. & Crighton, J. S. Locating transition states. *J. Chem. Phys.* **80**, 2464–2475 (1984).

47. Fischer, S. & Karplus, M. Conjugate peak refinement: an algorithm for finding reaction paths and accurate transition states in systems with many degrees of freedom. *Chem. Phys. Lett.* **194**, 252–261 (1992).

48. Refson, K. Variational density-functional perturbation theory for dielectrics and lattice dynamics. *Phys. Rev. B* **73**, 155114 (2006).

Acknowledgments

Author contributions

H.B.S. and H.Y.Y. proposed the idea. Z.R.W. performed the calculations. All authors discussed the results, wrote and commented on the manuscript at all stages.

Additional information

Competing financial interests: The authors declare no competing financial interests.

How to cite this article: Wang, Z., Yu, H. & Su, H. The transport properties of oxygen vacancy-related polaron-like bound state in HfOₓ. *Sci. Rep.* **3**, 3246; DOI:10.1038/srep03246 (2013).